A G Protein-Coupled Receptor Is a Plasma Membrane Receptor for the Plant Hormone Abscisic Acid

Xigang Liu, *et al.*

Science **315**, 1712 (2007);
DOI: 10.1126/science.1135882

The inheritable nature of CRISPR spacers supports the use of CRISPR loci as targets for evolutionary, typing, and comparative genomic studies (*9*, *17*–*19*). Because this system is reactive to the phage environment, it likely plays a significant role in prokaryotic evolution and ecology and provides a historical perspective of phage exposure, as well as a predictive tool for phage sensitivity. The CRISPR-*cas* system may accordingly be exploited as a virus defense mechanism and also potentially used to reduce the dissemination of mobile genetic elements and the acquisition of undesirable traits such as antibiotic resistance genes and virulence markers. From a phage evolution perspective, the integrated phage sequences within CRISPR loci may also provide additional anchor points to facilitate recombination during subsequent phage infections, thus increasing the gene pool to which phages have access (*20*). Because CRISPR loci are found in the majority of bacterial genera and are ubiquitous in Archaea (*5*, *13*, *21*), their study will provide new insights into the relation and codirected evolution between prokaryotes and their predators.

References and Notes

1. M. Breitbart, F. Rohwer, *Trends Microbiol.* **13**, 278 (2005).
2. S. Chibani-Chennoufi, A. Bruttin, M.-L. Dillmann, H. Brüssow, *J. Bacteriol.* **186**, 3677 (2004).
3. J. M. Sturino, T. R. Klaenhammer, *Nat. Rev. Microbiol.* **4**, 395 (2006).
4. H. Brüssow, *Annu. Rev. Microbiol.* **55**, 283 (2001).
5. R. Jansen, J. D. A. van Embden, W. Gaastra, L. M. Schouls, *Mol. Microbiol.* **43**, 1565 (2002).
6. A. Bolotin *et al.*, *Nat. Biotechnol.* **22**, 1554 (2004).
7. A. Bolotin, B. Quinquis, A. Sorokin, S. D. Ehrlich, *Microbiology* **151**, 2551 (2005).
8. F. J. M. Mojica, C. Díez-Villaseñor, J. García-Martínez, E. Soria, *J. Mol. Evol.* **60**, 174 (2005).
9. C. Pourcel, G. Salvignol, G. Vergnaud, *Microbiology* **151**, 653 (2005).
10. K. S. Makarova, N. V. Grishin, S. A. Shabalina, Y. I. Wolf, E. V. Koonin, *Biol. Direct* **1**, 7 (2006).
11. C. Lévesque *et al.*, *Appl. Environ. Microbiol.* **71**, 4057 (2005).
12. Information on materials and methods for the generation of phage-resistant mutants, engineering of CRISPR spacers (Figs. S4 and S5), and inactivation of *cas* genes is available on *Science* Online.
13. R. K Lillestøl, P. Redder, R. A. Garrett, K. Brügger, *Archaea* **2**, 59 (2006).
14. W. M. Russell, T. R. Klaenhammer, *Appl. Environ. Microbiol.* **67**, 4361 (2001).
15. K. S. Makarova, L. Aravind, N. V. Grishin, I. B. Rogozin, E. V. Koonin, *Nucleic Acids Res.* **30**, 482 (2002).
16. D. H. Haft, J. Selengut, E. F. Mongodin, K. E. Nelson, *PloS Comput. Biol.* **1**, e60 (2005).
17. P. M. A. Groenen, A. E. Bunschoten, D. van Soolingen, J. D. A. van Embden, *Mol. Microbiol.* **10**, 1057 (1993).
18. E. F. Mongodin *et al.*, *J. Bacteriol.* **187**, 4935 (2005).
19. R. T. DeBoy, E. F. Mongodin, J. B. Emerson, K. E. Nelson, *J. Bacteriol.* **188**, 2364 (2006).
20. R. W. Hendrix *et al.*, *Proc. Natl. Acad. Sci. U.S.A.* **96**, 2192 (1999).
21. J. S. Godde, A. Bickerton, *J. Mol. Evol.* **62**, 718 (2006).

22. We thank L. Bayer, C. Vos, and A.-C. Coûté-Monvoisin of Danisco Innovation, as well as J. Labonté and D. Tremblay of Université Laval for technical support, and E. Bech Hansen for discussions and critical review of the manuscript. Also, we thank T. R. Klaenhammer for providing the integration system. This work was supported by funding from Danisco A/S. Also, S. M. would like to acknowledge support from the Natural Sciences and Engineering Research Council of Canada (NSERC) Discovery Program. Sequences were deposited in GenBank, accession numbers EF434458 to EF434504.

Supporting Online Material

www.sciencemag.org/cgi/content/full/315/5819/1709/DC1
Materials and Methods
Figs. S1 to S5
References and Notes

29 November 2006; accepted 16 February 2007
10.1126/science.1138140

A G Protein–Coupled Receptor Is a Plasma Membrane Receptor for the Plant Hormone Abscisic Acid

Xigang Liu,[1,2] Yanling Yue,[1] Bin Li,[3] Yanli Nie,[1] Wei Li,[2] Wei-Hua Wu,[3] Ligeng Ma[1,2]*

The plant hormone abscisic acid (ABA) regulates many physiological and developmental processes in plants. The mechanism of ABA perception at the cell surface is not understood. Here, we report that a G protein–coupled receptor genetically and physically interacts with the G protein α subunit GPA1 to mediate all known ABA responses in *Arabidopsis*. Overexpressing this receptor results in an ABA-hypersensitive phenotype. This receptor binds ABA with high affinity at physiological concentration with expected kinetics and stereospecificity. The binding of ABA to the receptor leads to the dissociation of the receptor-GPA1 complex in yeast. Our results demonstrate that this G protein–coupled receptor is a plasma membrane ABA receptor.

Abscisic acid (ABA) is an important hormone that mediates many aspects of plant growth and development, particularly in response to the environmental stresses (*1*–*3*). Several components involved in the ABA signaling pathway have been identified (*4*). Two recent reports have shown that the nuclear RNA binding protein flowering time control protein (FCA) (*5*) and the chloroplast protein Mg chelatase H subunit (*6*) are ABA receptors (*6*). In contrast, several earlier experiments had suggested that extracellular perception is critical for ABA to achieve its functions (*7*–*9*). Thus, other ABA receptors, especially plasma membrane–localized receptors, may be the major players for perceiving extracellular ABA and mediating the classic ABA signaling responses.

Ligand-mediated signaling through G protein–coupled receptors (GPCRs) is a conserved mechanism for the extracellular signal perception at the plasma membrane in eukaryotic organisms (*10*). The GPCR-mediated signaling pathway plays a central role in vital processes such as vision, taste, and olfaction in animals (*11*). However, the higher plant *Arabidopsis thaliana* has only one canonical Gα (GPA1) subunit, one Gβ subunit, and two Gγ subunits (*12*–*16*). The significance of these subunits in plant systems is poorly understood; only one *Arabidopsis* putative GPCR protein (GCR1) has been characterized in plants (*17*–*20*), and no ligand has been defined for any plant GPCR.

To identify previously unrecognized GPCR proteins in *Arabidopsis*, we started by searching the *Arabidopsis* genome and found a gene (*GCR2*, GenBank accession code At1g52920) encoding a putative GPCR. Transmembrane structure prediction suggests that GCR2 is a membrane protein with seven transmembrane helices (fig. S1, A and B). The subsequent cellular localization analysis confirmed its plasma membrane localization in the transgenic plant root (fig. S1C). GCR2–yellow fluorescent protein (YFP) is detected in the membrane fraction isolated from the GCR2-YFP transgenic plant. Similar to GCR1 (*19*), GCR2 is mostly associated with the membrane fraction (fig. S1D). Furthermore, even after washing with detergent or a higher pH buffer, GCR2 is retained with the membrane fraction, suggesting that GCR2 is an integral membrane protein (fig. S1D).

One feature of the GPCR is its ability to interact with G protein to form a complex. To confirm the physical interaction between GCR2 and Gα, we used four different approaches to detect their interaction. We first used surface plasmon resonance spectroscopy to investigate the interaction between GCR2 and GPA1. For this purpose, we expressed and purified recombinant GCR2 and GPA1 proteins in bacteria (fig. S2). This in vitro assay clearly indicated that GPA1 is capable of binding to GCR2, whereas no binding activity was detected between GPA1 and bovine serum albumin (BSA) (fig. S3, A and B). The dissociation binding constant (K_d) for GCR2 and GPA1 is 2.1×10^{-9} M (fig. S3C).

[1]National Institute of Biological Sciences, 7 Science Park Road, Zhongguancun Life Science Park, Beijing 102206, China. [2]Laboratory of Molecular and Cellular Biology, Hebei Normal University, Shijiazhuang, Hebei 050016, China. [3]State Key Laboratory of Plant Physiology and Biochemistry, College of Biological Sciences, China Agricultural University, Beijing 100094, China.

*To whom correspondence should be addressed. E-mail: maligeng@nibs.ac.cn

The commonly used yeast two-hybrid system does not work for the GCR2-GPA1 interaction assay because of their membrane localization, so we used a split-ubiquitin system (*21*) instead to investigate the GCR2-GPA1 interaction in yeast. This assay confirmed the reported interaction of the full-length GCR1 with GPA1 (*19*), and the full-length GCR2 also interacted with GPA1 (fig. S4A). The interaction was abolished when the C terminus of the receptor was blocked by fusing the ubiquitin fragment (CubPLV) to the C terminus of GCR2 (fig. S4A). We also found that the C terminus of GCR2 ($C_{290–401}$, containing the free C terminus and the predicted third cytoplasmic loop) interacted with GPA1, whereas the N terminus ($N_{1–289}$) of GCR2 did not (fig. S4, B and C), indicating that the C terminus of GCR2 is necessary and sufficient for its interaction with GPA1.

Bimolecular fluorescence complementation was used to detect the interaction between GCR2 and GPA1 in plant cells. GCR2 and GPA1 interacted in *Arabidopsis* protoplasts (Fig. 1A). Removal of the C terminus of GCR2 ($C_{290–401}$) abolished the interaction (Fig. 1, A and B). This indicated that the interaction between GCR2 and GPA1 is specific and that the C terminus of GCR2 is necessary for its interaction with GPA1. We also confirmed their in vivo interaction by a coimmunoprecipitation assay. GCR2 and GPA1 can be coimmunoprecipitated; and we could detect GPA1 in the immunocomplex precipitated with an antibody to FLAG from GCR2-FLAG transgenic plants (Fig. 1C). Thus, results from four distinct assays all supported the interaction between GCR2 and GPA1.

To analyze the function of GCR2 in *Arabidopsis*, we characterized three independent *Arabidopsis* lines harboring the transferred DNA insertions in the *GCR2* locus, *gcr2-1*, *gcr2-2*, or *gcr2-3* (fig. S5). Transcript analysis by reverse transcription polymerase chain reaction (RT-PCR) detected no full-length *GCR2* transcripts in any of the three mutant alleles, but all had the truncated transcripts (fig. S5).

Arabidopsis seeds require desiccation or dormancy to prevent premature germination before harvesting. The freshly harvested wild-type seeds seldom germinate; however, freshly harvested seeds from all three alleles of *gcr2* plants germinated well under the same condition (Fig. 2A), indicating that the seeds from *gcr2* mutants lost seed dormancy. The seed dormancy is mainly controlled by phytohormone ABA. This result suggested that *gcr2* mutants are defective in ABA signaling. We therefore reasoned that the mutations in *GCR2* lead to a decreased sensitivity to ABA. We examined other ABA responses in both wild-type and *gcr2* plants. We first checked the effect of *GCR2* mutations on seed germination in the presence of ABA and found that all three *gcr2* mutants were insensitive, whereas the seeds from GCR2 overexpressor lines were hypersensitive to the ABA-inhibition compared with the wild-type seeds (Fig. 2B). We also found that the seedling growth inhibition by ABA was substantially reduced in the *gcr2* mutants, but increased in GCR2 overexpressor lines compared with that of the wild type (Fig. 2C). In the absence of ABA, the *gcr2* seedlings developed normally and were indistinguishable from the wild-type seedlings (Fig. 2C). ABA mediates plant development by controlling the expression of ABA-mediated genes, and we thus compared the expression of ABA marker genes in wild-type and *gcr2* plants. Three well-known ABA marker genes, *RD29A*, *KIN1*, and *ABI5*, were tested. This analysis confirmed that the expression of ABA marker genes was substantially repressed in the *gcr2* mutants (fig. S6).

The ABA-induced closing and ABA-inhibited opening of stomata are classical ABA responses. We observed that both ABA-induced stomata closing and ABA-inhibited stomata opening were insensitive in *gcr2* compared with *gcr2* sensitivity in wild-type plants (Fig. 2, D and E), and the stomata width is larger in *gcr2* plants than in wild-type plants (Fig. 2E). ABA regulates inward K^+ (K^+_{in}) channels to control the stomatal aperture (*22*, *23*). To determine whether GCR2 mediates the ABA regulation of K^+_{in} channels in stomatal guard cells, we applied patch-clamping techniques to analyze the whole-cell K^+_{in} currents in guard cells from wild-type and *gcr2-1* plants. ABA inhibited K^+_{in} currents in wild-type guard cells but had no effect on the K^+_{in} currents in *gcr2-1* guard cells (Fig. 2F), thus indicating the involvement of GCR2-mediated K^+_{in} in ABA-induced stomatal closure. We also found that stomata from GCR2-overexpressing plants were hypersensitive to ABA-induced closure compared with the sensitivity of the wild-type plants (Fig. 2G). The stomata closure defects resulted in a greater water loss in the leaves of the three *gcr2* alleles compared with that in wild-type leaves, whereas water loss was reduced in *GCR2*-overexpressing plant leaves (fig. S7). All of these results indicate that *gcr2* plants are insensitive to ABA, whereas *GCR2*-overexpressing plants are hypersensitive to ABA, demonstrating the involvement of GCR2 in all major ABA responses in *Arabidopsis*.

The *gcr2* plants exhibit all known major ABA defects. The GPA1 null mutant (*gpa1*) is also defective in ABA-induced stomatal opening and inward K^+-channel regulation in guard cells (*22*). Expression pattern analysis shows that *GCR2* and *GPA1* share a very similar expression pattern (fig. S8, A and B). We also examined the functional significance of GCR2-GPA1 interaction by checking the ABA response in the *gcr2gpa1* or overexpressor of *GCR2* or *GPA1* in different genetic background using stomatal closure as an assay. We found that GPA1 was involved in both ABA-controlled stomatal opening and closing (Fig. 2E and fig. S8, C to E). The defect exhibited by *gcr2gpa1* in ABA-induced stomatal closure was similar to the defect exhibited by *gcr2* or *gpa1* (fig. S8C). Transgenic lines overexpressing *GCR2* or *GPA1* were hypersensitive to the ABA response; however, the effects caused by the overexpression of *GCR2* or *GPA1* were dependent on GPA1 or GCR2, respectively (fig. S8, B, C, and E), indicating that GCR2 and GPA1 function together to transduce the ABA signal.

Given that *gcr2* exhibits defects in all known ABA responses and that GCR2 is a plasma

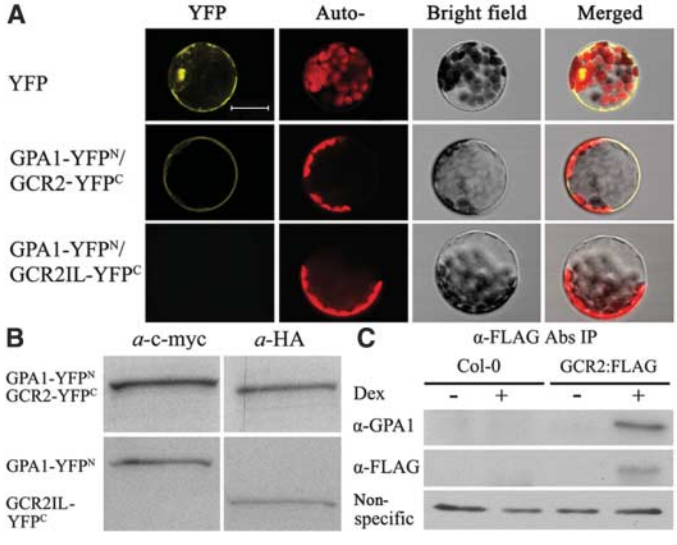

Fig. 1. Physical interaction between GCR2 and GPA1. (**A**) Bimolecular fluorescence complementation assays indicating the interaction of GCR2: hemagglutinin (HA) with a C-terminal HA tag, but not the corresponding C-terminal deletion construct GCR2IL:HA ($N_{1–289}$) with GPA1 in vivo. Auto-, autofluorescence. The scale bar represents 20 μm. (**B**) The GCR2:HA-YFC^C, GCR2IL:HA-YFP^C, and GPA1:cMYC-YFP^N proteins were expressed in the protoplast. Proteins from *Arabidopsis* protoplasts expressing GCR2:HA-YFC^C, GCR2IL:HA-YFP^C, or GPA1:cMYC-YFP^N were extracted and the sample was analyzed on a 12% SDS–polyacrylamide gel electrophoresis gel. GCR2 or GPA1 was detected with the use of anti-HA for GCR2-YFC^C or GCR2IL-YFP^C, or anti–c-Myc for GPA1-YFP^N. (**C**) Coimmunoprecipitation (Co-IP) assays verifying the interaction between GCR2 and GPA1 in planta. Total proteins from wild-type (Col-0) and GCR2:FLAG transgenic plants were used for in vivo Co-IP with antibodies to FLAG. Immunoprecipitated proteins were probed with antibodies (α) to GPA1 and to FLAG. An anti-FLAG cross-reacting band is shown as the loading control.

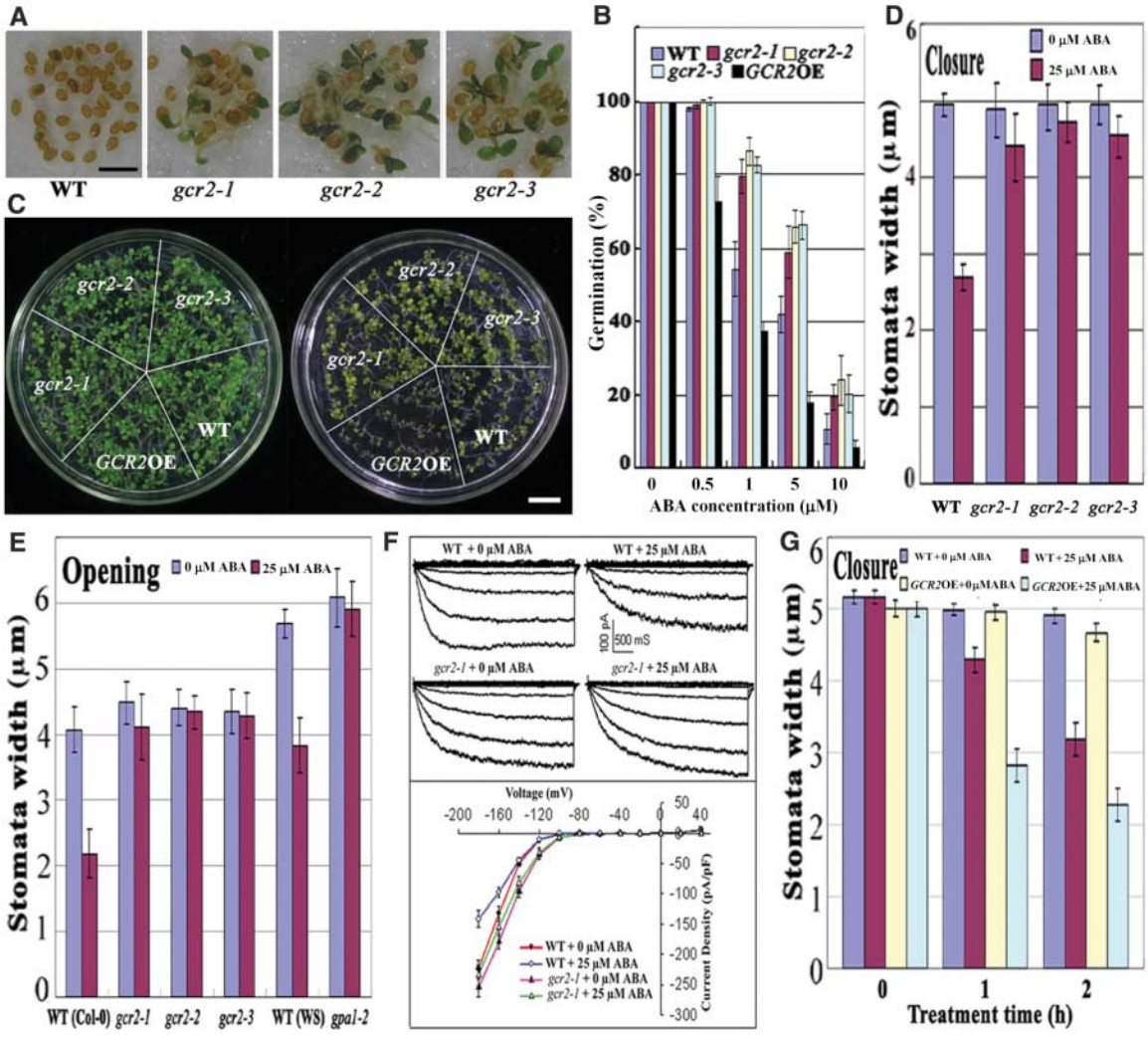

Fig. 2. The *gcr2* mutants exhibit all known ABA defects. (**A**) The *gcr2* seeds lose the seed dormancy observed in the wild type (WT). Freshly harvested seeds germinated on water-soaked filter paper for 7 days. The scale bar represents 2 mm. (**B**) The *gcr2* seeds are insensitive to ABA-inhibited seed germination (mean ± SD; $n = 4$). The germination percentage was determined 3 days after growing in 1/2 Murashige and Skoog (MS) media. (**C**) The seedling development in *gcr2* is insensitive to ABA. Seeds were grown on 1/2 MS media with (right) or without (left) 0.3 μM ABA for 10 days. *GCR2*OE, *GCR2* overexpressor line. The scale bar represents 1 cm. (**D**) The *gcr2* plants show defects in ABA-induced stomatal closure (mean ± SD; $n = 3$). (**E**) The *gcr2* and *gpa1* plants are insensitive to ABA for stomatal opening (mean ± SD; $n = 3$). WS, Wassilewskija. (**F**) The inward K^+ channel in *gcr2* guard cells is insensitive to ABA. The data in the graph (bottom) are presented as mean ± SE ($n = 4$, 3, 5, and 6 for wild type, wild type+ABA, *gcr2-1*, and *gcr2-1*+ABA, respectively). (**G**) Overexpressor of *GCR2* confers increased ABA sensitivity for stomatal closure (mean ± SD; $n = 3$).

membrane receptor, we examined whether GCR2 is an ABA receptor. For this purpose, we first checked whether GCR2 could bind ABA. We observed that ABA bound to GCR2 but did not bind to denatured GCR2 protein (Fig. 3A). As a positive and negative control, ABA also bound to FCA but not BSA or GPA1 (Fig. 3A). The binding of ABA to GCR2 protein is dependent on pH, and the optimum pH is between 7.0 and 7.5 (fig. S9). Stereospecificity of GCR2 binding to the biologically active (+)-ABA was tested in competition assays. Trans-ABA and (–)-ABA analogs did not compete for the GCR2-binding site (Fig. 3B).

The specific binding of ABA to purified GCR2 could be saturated with increasing amounts of ABA (Fig. 3C). Scatchard plot analysis exhibits a linear pattern (Fig. 3D), suggesting a single binding site for ABA in GCR2. The equilibrium dissociation constant (K_d) for the GCR2-ABA complex is 20.1 nM (Fig. 3D), which is consistent with the physiological concentration range of ABA in plants.

Ligand binding to the GPCR induces the dissociation of the GPCR–G protein complex to release Gα and the Gβγ dimer, thus activating the downstream signaling events (*16*, *24*). To test whether the binding of ABA to GCR2 could dissociate the GCR2-GPA1 complex, we used the split-ubiquitin system to reconstitute this initial ABA signaling event in yeast. Application of the physiologically active form of ABA [(±)-ABA or (+)-ABA] indeed disrupted the GCR2-GPA1 interaction, whereas the physiologically inactive forms of ABA analogs [(–)-ABA or trans-ABA] did not affect the interaction between GCR2 and GPA1, as indicated in the coimmunoprecipitation assay (Fig. 3E). This result again clearly confirmed that the binding of ABA to GCR2 is stereospecific.

In the split-ubiquitin yeast protein interaction assay, the downstream reporter genes (*HIS3*, *ADE2*, and *lacZ*) were activated if the two assayed proteins interacted with each other (*21*). We reasoned that the binding of ABA to GCR2 could repress the expression of reporter genes as a result of the dissociation of GCR2 and GPA1. This prediction was verified (fig. S10). The addition of a physiologically active form of ABA repressed *lacZ* expression, whereas physiologically inactive forms of ABA [(–)-ABA or trans-ABA] did not (fig. S10). As a control, ABA did not affect the expression of the reporter gene in a reconstituted K^+ ATPASE1 (KAT1)–KAT1 pathway in the same split-ubiquitin system (fig. S10). In addition, the expression of another two reporter genes, *HIS3* and *ADE2*, was necessary for yeast proliferation in a selection medium. The addition of ABA substantially repressed the proliferation of yeast expressing GCR2 and GPA1, but did not affect yeast proliferation in expressing KAT1-KAT1 system (Fig. 3E). Together, these results indicated that the effect of ABA on reporter gene expression was specific for the GCR2-GPA1 interaction, further supporting that the binding of ABA to GCR2 results in the dissociation of the GCR2-GPA1 complex.

Terrestrial plants are immobile and incapable of escaping unfavorable environmental conditions such as drought or cold. Instead, they rely heavily on ABA to survive these conditions. Thus, how plants perceive and transduce the

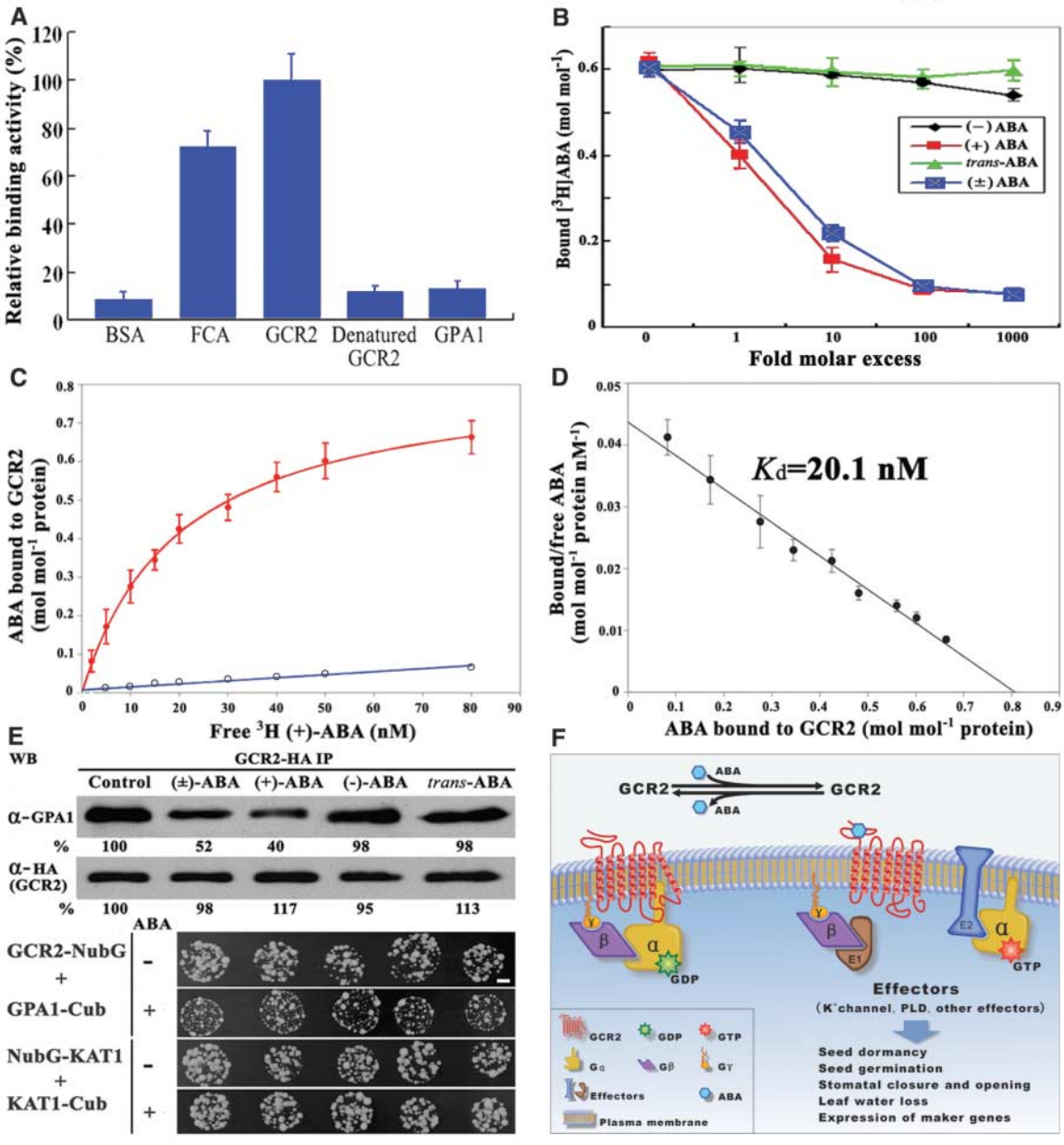

Fig. 3. Binding of ABA to GCR2. (**A**) ABA binds to the purified GCR2 protein (mean ± SD; n = 3). (**B**) GCR2 binding of ABA is stereospecific (mean ± SD). (**C**) ABA binding to GCR2 behaves according to saturation kinetics. The specific and nonspecific bindings are represented by top and bottom curves, respectively (mean ± SD; n = 5). (**D**) Scatchard plot analysis of ABA binding shows a linear relationship with the square of the correlation coefficient $r^2 = 0.99$, and maximum binding is 0.8 mol mol^{-1} protein with K_d = 20.1 nM (mean ± SD; n = 5). (**E**) ABA disrupts the GCR2-GPA1 interaction in yeast. (Top) Co-IP assay. After 10 μM ABA was added to the medium for 20 min, proteins were isolated. The relative intensity of the immunosignal to the control is indicated by the number below each band. WB, Western blot. (Bottom) Yeast growth assay. The proliferation was observed 7 days after the addition of 10 μM (±)-ABA and 1 mM methionine. NubG, ubiquitin N terminus *I* 13 *G* mutation. The scale bar represents 2 mm. (**F**) Schematic model for GCR2-mediated ABA signaling pathway. GDP, guanosine diphosphate; GTP, guanosine 5′-triphosphate; PLD, phospholipase D.

ABA signal is a fundamental question. It has been shown that GPA1 was involved in ABA-mediated stomatal response and seed germination (*19*, *22*, *25*); a putative GPCR GCR1 interacted with GPA1 to negatively regulate ABA signaling (*19*). We now describe the characterization of a new GPCR, GCR2, in *Arabidopsis*. We conclude that GCR2 is a major ABA receptor on the basis of the following evidence: (i) Loss-of-function *gcr2* exhibits all known ABA defects; (ii) an overexpressor of GCR2 shows an ABA-hypersensitive phenotype; (iii) GCR2 binds ABA with a high affinity and reasonable dissociation constants, and the binding is stereospecific and abides by receptor kinetics; (iv) GCR2 is localized in the plasma membrane; (v) GCR2 genetically and physically interacts with GPA1; and (vi) the binding of ABA to GCR2 disrupts GCR2-GPA1 interaction. Notably, the *gcr2* mutants still display ABA responses. This may be due to the weak nature of the mutations (fig. S5) or functional redundancy with GCR2-related proteins, given that there are two other *GCR2* homologous genes in the *Arabidopsis* genome. Consistent with this latter possibility, the semidominant phenotype and partial complementation of *gcr2* by *GCR2* cDNA expression (fig. S11) suggests the possible interference between GCR2 and its homologs.

The following model of ABA signaling can be envisaged. A GPCR, GCR2, which is a plasma membrane–localized ABA receptor, interacts with the Gαβγ complex. Binding of ABA to GCR2 results in the release of the G protein and dissociation of the heterotrimeric complex into Gα and the Gβγ dimer to activate downstream ABA effectors and to trigger the ABA responses (Fig. 3F). Thus, our results identified an ABA receptor and its target protein, a heterotrimeric G protein.

References and Notes

1. R. R. Finkelstein, S. L. Gampala, C. D. Rock, *Plant Cell* **14**, S15 (2002).
2. J. Leung, J. Giraudat, *Annu. Rev. Plant Physiol. Plant Mol. Biol.* **49**, 199 (1998).
3. J. I. Schroeder, J. M. Kwak, G. J. Allen, *Nature* **410**, 327 (2001).
4. J. K. Zhu, *Annu. Rev. Plant Biol.* **53**, 247 (2002).
5. F. A. Razem, A. El-Kereamy, S. R. Abrams, R. D. Hill, *Nature* **439**, 290 (2006).
6. Y. Y. Shen *et al.*, *Nature* **443**, 823 (2006).
7. B. E. Anderson, J. Ward, J. Schroeder, *Plant Physiol.* **104**, 1177 (1994).
8. S. Gilroy, R. Jones, *Proc. Natl. Acad. Sci. U.S.A.* **89**, 3591 (1992).
9. E. Jeannette *et al.*, *Plant J.* **18**, 13 (1999).

10. K. L. Pierce, R. T. Premont, R. J. Lefkowitz, *Nat. Rev. Mol. Cell Biol.* **3**, 639 (2002).
11. A. M. Spiegel, L. S. Weinstein, *Annu. Rev. Med.* **55**, 27 (2004).
12. H. Ma, M. Yanofsky, E. M. Meyerowitz, *Proc. Natl. Acad. Sci. U.S.A.* **87**, 3821 (1990).
13. H. Ma, *Plant Mol. Biol.* **26**, 1611 (1994).
14. M. G. Mason, J. Botella, *Proc. Natl. Acad. Sci. U.S.A.* **97**, 14784 (2000).
15. M. G. Mason, J. R. Botella, *Biochim. Biophys. Acta* **1520**, 147 (2001).
16. A. M. Jones, S. A. Assmann, *EMBO Rep.* **5**, 572 (2004).
17. S. Plakidou-Dymock, D. Dymock, R. Hooley, *Curr. Biol.* **8**, 315 (1998).
18. G. Colucci, F. Apone, N. Alyeshmerni, D. Chalmers, M. J. Chrispeels, *Proc. Natl. Acad. Sci. U.S.A.* **99**, 4736 (2002).
19. S. Pandey, S. M. Assmann, *Plant Cell* **16**, 1616 (2004).
20. S. M. Assmann, *Science* **310**, 71 (2005).
21. P. Obrdlik *et al.*, *Proc. Natl. Acad. Sci. U.S.A.* **101**, 12242 (2004).
22. X.-Q. Wang, H. Ullah, A. M. Jones, S. M. Assmann, *Science* **292**, 2070 (2001).
23. J. M. Ward, Z. M. Pei, J. I. Schroeder, *Plant Cell* **7**, 833 (1995).
24. S. R. Sprang, *Annu. Rev. Biochem.* **66**, 639 (1997).
25. S. Pandey, J. G. Chen, A. M. Jones, S. M. Assmann, *Plant Physiol.* **141**, 243 (2006).
26. We thank D. Y. Sun for his support; X. W. Deng and J. M. Zhou for their comments and discussion; W. Frommer and P. Obrdlik for making the split-ubiquitin system available; J. Kuala for making the split-YFP system available; J. Chai for his technical assistance and advice for the protein purification; and D. Zhang, Y. Shen, and F. Razem for their suggestions on the ABA binding assay. This work was supported by the Ministry of Science and Technology of China (to L.M., 2003AA210120), National Science Foundation of China for Outstanding Young Scientists (to L.M., 30025024) and the Chinese National Key Basic Research Project (to W.W., 2006CB100100).

Supporting Online Material
www.sciencemag.org/cgi/content/full/1135882/DC1
Materials and Methods
Figs. S1 to S11
References

3 October 2006; accepted 24 January 2007
Published online 8 March 2007;
10.1126/science.1135882
Include this information when citing this paper.

Tunability and Noise Dependence in Differentiation Dynamics

Gürol M. Süel,[1] Rajan P. Kulkarni,[2] Jonathan Dworkin,[3] Jordi Garcia-Ojalvo,[4] Michael B. Elowitz[2]*

The dynamic process of differentiation depends on the architecture, quantitative parameters, and noise of underlying genetic circuits. However, it remains unclear how these elements combine to control cellular behavior. We analyzed the probabilistic and transient differentiation of *Bacillus subtilis* cells into the state of competence. A few key parameters independently tuned the frequency of initiation and the duration of competence episodes and allowed the circuit to access different dynamic regimes, including oscillation. Altering circuit architecture showed that the duration of competence events can be made more precise. We used an experimental method to reduce global cellular noise and showed that noise levels are correlated with frequency of differentiation events. Together, the data reveal a noise-dependent circuit that is remarkably resilient and tunable in terms of its dynamic behavior.

Three aspects of genetic circuits control dynamic cellular behaviors: the circuit architecture or pattern of regulatory interactions among genetic elements; quantitative parameter values, such as promoter strengths; and stochastic fluctuations, or "noise," associated with the concentration of cellular components. A fundamental biological question is how these three aspects of genetic circuits combine to determine cellular behavior, its variability, and its potential to evolve (*1*).

Competence in *B. subtilis* is a stress response that allows cells to take up DNA from the environment (*2*, *3*). Differentiation into competence is transient (Fig. 1A) (*4*). The genetic basis for this behavior is a circuit involving *comK* and *comS* (Fig. 1B). The transcription factor ComK is necessary and sufficient for differentiation into competence (*5*, *6*). ComK positively autoregulates its own expression but is degraded by the ClpP-ClpC-MecA protease complex (Fig. 1B) (*7*–*9*). ComS competitively inhibits this degradation and is repressed in competent cells, forming a negative feedback loop (*4*, *10*, *11*). The circuit operates as an excitable system in which a relatively small perturbation induces a larger and stereotyped response, as occurs with action potentials in neurons, for example (*4*, *12*). Competence events occur only in a fraction of cells and may be driven by noise in underlying circuit components (*4*, *7*, *8*, *13*).

Two key characteristics of competence are its probability of initiation, P_{init}, and the mean duration of transient competence events, τ_{comp} (Fig. 1A). P_{init} denotes the chance per cell division that an individual cell will become competent. Competence events can be quantified by automated time-lapse fluorescence microscopy using fluorescent reporter genes under the control of the ComK-specific *comG* promoter and the *comS* promoter (denoted P_{comG} and P_{comS}, respectively) (*4*).

Two parameters that are expected to affect the behavior of the circuit are the basal expression rates of *comK* and *comS*, denoted by α_K and α_S, respectively (Fig. 1B and Eq. S1). To manipulate these parameters, we chromosomally integrated an additional copy of either *comS* or *comK* under the control of an inducible promoter, denoted P_{hyp}, generating the Hyper-α_S and Hyper-α_K

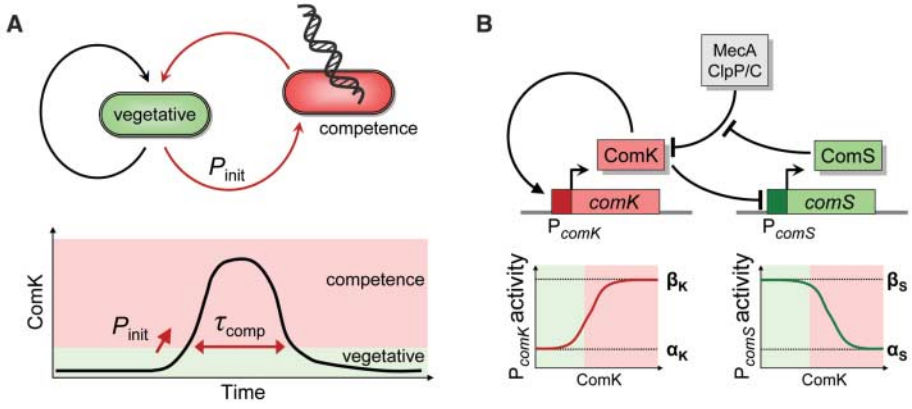

Fig. 1. Competence is a probabilistic and transient differentiation process regulated by a genetic circuit. (**A**) The rate of entering the competent state from the vegetative state is denoted by P_{init}. The amount of time spent in the competent state is denoted by τ_{comp}. The ComK transcription factor concentration is high (pink region) when cells are competent and low (green region) when they are growing vegetatively. (**B**) Map of the core competence circuitry. Key features include positive transcriptional autoregulation of *comK* and a negative feedback loop in which ComK inhibits (possibly indirectly) expression of ComS, which in turn interferes with degradation of ComK. The graphs below the P_{comK} and P_{comS} promoters define parameters used in the text: Expression rates change from α_K to β_K and β_S to α_S respectively, as ComK concentration increases during competence.

[1]Green Center Division for Systems Biology and Department of Pharmacology, University of Texas Southwestern Medical Center, Dallas, TX 75390, USA. [2]Division of Biology and Department of Applied Physics, California Institute of Technology, Pasadena, CA 91125, USA. [3]Department of Microbiology, College of Physicians and Surgeons, Columbia University, New York, NY 10032, USA. [4]Departament de Física i Enginyeria Nuclear, Universitat Politècnica de Catalunya, Colom 11, E-08222 Terrassa, Spain.

*To whom correspondence should be addressed. E-mail: melowitz@caltech.edu